Master of Science Thesis in Electrical Engineering
Department of Electrical Engineering, Linköping University, 2021

Tyre Performance Estimation during Normal Driving

Marcus Grip

Master of Science Thesis in Electrical Engineering

Tyre Performance Estimation during Normal Driving

Marcus Grip

LiTH-ISY-EX--21/5391--SE

Supervisor: **Pavel Anistratov**
ISY, Linköpings universitet
Jesper Otterholm
NIRA Dynamics AB

Examiner: **Erik Frisk**
ISY, Linköpings universitet

Division of Vehicle Systems
Department of Electrical Engineering
Linköping University
SE-581 83 Linköping, Sweden

Abstract

Driving with tyres not appropriate for the actual conditions can not only lead to accidents related to the tyres, but also cause detrimental effects on the environment via emission of rubber particles if the driving conditions are causing an unexpectedly high amount of tread wear. Estimating tyre performance in an online setting is therefore of interest, and the feasibility to estimate friction performance, velocity performance, and tread wear utilizing available information from the automotive grade sensors is investigated in this thesis.

For the friction performance, a trend analysis is performed to investigate the correlation between tyre stiffness and friction potential. Given that there is a correlation, a model is derived based on the trend having a stiffness parameter as an input in order to predict the friction performance. Tendencies for a linear trend is shown, and a linear regression model is fitted to data and is evaluated by calculating a model fit and studying the residuals. Having a model fit of 80%, the precision of the expected values stemming from the proposed model is concluded to be fairly low, but still enough to roughly indicate the friction performance in winter conditions.

A tread wear model that can estimate the amount of abrasive wear is also derived, and the proposed model only utilizes available information from the automotive grade sensors. Due to the model having a parameter that is assumed to be highly tyre specific, only a relative wear difference can be calculated. The model is evaluated in a simulation environment by its ability to indicate if a tyre is under the influence of a higher wear caused by a higher ambient temperature. The results indicates that the model is insufficient in an online setting and cannot accurately describe the phenomena of softer tyres having a larger amount of wear caused by a high ambient temperature compared to stiffer tyres.

Lastly, a double lane change test (ISO 3888-2) is conducted to determine the critical velocity for cornering manoeuvres, which defines the velocity performance. The test was executed for six different sets of tyres, two of each type (winter, all-season, and summer). The approach to estimate the velocity performance in an online setting is analogue to that of the friction performance, and a trend analysis is performed to investigate the correlation between longitudinal tyre stiffness and the critical velocity. The results are rather unexpected and shows no substantial differences in velocity performance, even though the tyre-road grip felt distinctively worse for the softer tyres according to the driver. It is concluded that the bias stemming from the professional driver's skills might have distorted the results, and that another approach might need to be considered in order to estimate this performance.

Acknowledgements

First of all, I would like to thank my supervisor at NIRA Dynamics, Jesper Otterholm, not only for the immense commitment, but also for the many insightful and rewarding discussions. I would also like to extend my gratitude to the entire TGI-team for their continuous support, positive attitude, and interest in this thesis. Many thanks to Pavel Anistratov at ISY for the guidance and valuable input during the writing process. Lastly, I would like to express my gratitude to my examiner, Erik Frisk, at ISY for his time and effort.

Linköping, May 2021
Marcus Grip

Contents

Notation

Notations

Notation	Meaning
F_x	Longitudinal force
F_y	Lateral force
F_z	Normal force
F_c	Centripetal force
σ_x	Longitudinal slip
α	Slip angle
β	Body side-slip angle
δ_1	Steering angle (front)
ϵ	Residual
R_e	Effective radius
r	Corner radius
R^2	Coefficient of determination
Ω	Angular velocity
Ω_0	Rotational velocity of the freely rolling wheel
V	Velocity vector
V_x	Longitudinal velocity component
V_y	Lateral velocity component
V_{sx}	Longitudinal slip velocity
V_{sy}	Lateral slip velocity
V_{max}	Critical velocity
ρ	Normalized traction force
ρ_x	Normalized longitudinal force
ρ_y	Normalized lateral force
$\mu_{x,max}$	Longitudinal friction potential
$\mu_{y,max}$	Lateral friction potential
C_x	Longitudinal stiffness
C_y	Lateral stiffness
C_{xr}	Compensated longitudinal stiffness

Notations

Notation	Meaning
I	Amount of tread wear
I_{rel}	Relative wear change
γ	Abrasion per unit energy dissipation
W_x	Work done by friction in the longitudinal direction
W_y	Work done by friction in the lateral direction
w_x	Longitudinal energy rate
w_y	Lateral energy rate
m	Vehicle's mass
a_x	Longitudinal acceleration
a_y	Lateral acceleration
$\dot{v}$	Tangential acceleration
$\ddot{\psi}$	Yaw-acceleration
J_z	Moment of inertia about centre of gravity
l_f	Distance from the front axle to the centre of gravity
l_r	Distance from the rear axle to the centre of gravity
T_{amb}	Ambient temperature
T_{tyre}	Tyre temperature

Abbreviations

Abbreviation	Meaning
ABS	Anti-lock Braking System
CAN	Controller Area Network
COG	Centre of Gravity
EPS	Electronic Power Steering
ESC	Electronic Stability Control
IMU	Inertial Measurement Unit
ISO	International Organization for Standardization
TGI	Tire Grip Indicator

1 Introduction

1.1 Background

Retrieving tyre characteristics based on the information available on the vehicle Controller Area Network (CAN) bus, is of high interest since the risk of accidents increases significantly if the vehicle is equipped with the wrong tyres for the actual driving conditions [1]. Research has, for example, been carried out to identify different types of tyres (summer/winter) on the vehicle by utilizing image processing [2]. Having identification systems that can classify the type of tyres (summer/winter) have been desirable to help improving the overall safety, since manual inspection sometimes can overlook unsuitable tyre types [3].

It is, however, interesting to look at certain performance indicators instead of just the tyre label (summer/winter), since in reality the label does not necessarily mean that the tyre will perform well and be a safe choice for the driver, even if it is specified for the season it is being used in [4]. NIRA Dynamics AB is therefore interested in the potential information that can be retrieved about the tyres of passenger vehicles online during normal driving. This information could be used to warn the driver if the tyres are not suitable for the driving conditions and thus help preventing accidents in traffic. From environmental perspectives it is also beneficial to warn if the driving conditions are causing an unexpectedly high amount of tread wear, since tyre wear has negative impacts on the environment via emission of tyre rubber particles [5]. The information could also be utilized to gain a further understanding of how different types of tyres behave in various conditions.

1.2 Objective

The objective of this master's thesis is to study the feasibility to estimate performance indicators for the tyres online during normal driving, by utilizing information from the automotive grade sensors available in common passenger vehicles and the NIRA Dynamics product Tire Grip Indicator (TGI). The goal is to improve the amount of valuable tyre information NIRA Dynamics is currently able to extract from the automotive grade sensors and their product TGI. The information NIRA is specifically interested in is: the tyres' friction performance, their velocity performance and the rate of tread wear. These will all be separately discussed in Chapter 3, 4 and 5.

1.3 Research Questions

This master's thesis aims to answer the following research questions:

1. Can information available from the automotive grade sensors be used to predict the tyres' friction performance in winter conditions?
2. Can information available from the automotive grade sensors be used to predict the tyres' velocity performance?
3. Can a wear model, that only utilizes available information from the automotive grade sensors, be used to indicate if the tyres are under the influence of a higher wear caused by a higher ambient temperature?

1.4 Outline

This master's thesis consists of 7 chapters in total. In Chapter 1 a short introduction to the problem is given, and an objective is defined. A brief discussion of previous work related to the problem is also presented, and a short description of a general methodology is given; In Chapter 2 general underlying theory regarding the pneumatic tyre and tyre wear is presented; The friction performance is defined in Chapter 3 and a strategy for estimating friction performance is suggested; In Chapter 4 a proposed tread wear model is given and a simulation environment is defined; The velocity performance is defined in Chapter 5 and an approach is proposed along with a description of the practical data acquisition; In Chapter 6 the obtained results are presented and discussed; A summary of the thesis along with conclusions that can be made given the results is presented in Chapter 7.

1.5 Previous Work

The objective formulated in Chapter 1.2 suggests that information about the tyre behaviour needs to be retrieved. Previous research in the area of online estimation of tyre performance does, however, seem to be rather limited. Since the

tyres are generating essential forces for vehicle motion (as they are the only contact point between the ground and the vehicle), tyre behaviour is of interest for vehicle simulations as well [6]. It is common to describe the behaviour by estimating tyre models, and there are two main strategies often used in literature. One of the strategies commonly used is physical models such as the brush-type model, which was mainly used before more empirical methods became popular [7]. The brush-type model utilizes rather simple expressions for the slip and the tyre-force relations, and the trade-off for being a relatively simple model is accuracy.

A more accurate way of modelling tyres is by utilizing empirical methods, such as Pacejka's tyre model (often referred to as Magic Formula), which has a higher accuracy for higher slip ratios compared to the brush-type [8]. This method requires a large amount of experimental data about the tyres for estimating the model parameters, and there are different methods of estimating these parameters efficiently with a high accuracy [6]. Research shows that it is possible to use Dual Unscented Kalman Filter to estimate the lateral forces of the tyre [9]. These forces can then be used to determine/identify the parameters for the Magic Formula tyre model. This method of estimating the model parameters eliminates the need of having a large amount of experimental tyre data.

The previous work that has been described so far primarily uses methods for estimating model parameters in an offline setting. Published research shows that it is possible to identify tyre model parameters online [10]. It is, however, not feasible to identify model parameters for complex models since the time for estimating parameters is very short during continuous driving.

When studying tyre wear there are a few wear models that show a high amount of presence in literature. The two simple physical wear models Archard's wear model and Schallamach's model seem to be the most common when estimating the amount of wear. Both rely on relatively simple expressions with a few sets of parameters. There are, however, more advanced models to predict the tyre wear. Research shows that an advanced wear model, that takes directional effects and history dependency of abrasion into consideration, yield good results for predicting rubber abrasion [11]. Research of estimating tyre wear in an online setting is, however, very limited.

1.6 Methodology

As described in Chapter 1.5, methods for studying and predicting tyre behaviour by estimating extensive tyre models exist, which are often utilized in simulation environments. In this master's thesis, a more practical-oriented approach is considered, due to the fact that the objective requires online prediction of the tyres' performance during normal driving. It can also be assumed that no experimental data associated with the specific tyres the vehicle is equipped with is available.

Signals available on the CAN bus and information from TGI will therefore solely be used along with practical data acquisition, which will be further discussed in Chapter 5.3 .

The signals that are available from the automotive grade sensors, and that will be used for the online estimation of the performance indicators mentioned in Chapter 1.2 can be seen in Table 1.1.

Source	Signal	Unit
IMU	Lateral Acceleration	m/s^2
IMU	Longitudinal Acceleration	m/s^2
IMU	Yaw Rate	rad/s
Engine	Engine Speed	rad/s
Wheel Sensors	Wheel Speed Front Left	rad/s
Wheel Sensors	Wheel Speed Front Right	rad/s
Wheel Sensors	Wheel Speed Rear Left	rad/s
Wheel Sensors	Wheel Speed Rear Right	rad/s
Wheel Sensors	Wheel Angle Front	rad
Wheel Sensors	Wheel Angle Rear	rad
EPS	Steering Wheel Angle	rad

Table 1.1: *The signals available from the automotive grade sensors are presented in the table.*

1.6.1 Database

For validation purposes, a database with logged data from numerous different test drives of different tyres and passenger vehicles in various driving conditions, is available at NIRA. The data mainly contains logged signals from the automotive grade sensors and TGI. For every test drive, information about the driving style, route, vehicle velocity, vehicle type, ambient temperature, weather condition, and road surface (type of surface) is known.

1.6.2 Tire Grip Indicator

The product Tire Grip Indicator is a software solution developed by NIRA and requires no additional sensors since it utilizes the existing information provided by the automotive grade sensors. TGI essentially monitors the tyre-road friction, the friction between the tyres and the road, and works during normal driving, i.e., it is capable of estimating the friction potential long before the maximum available friction is utilized. In order to estimate the available friction under normal conditions, tyre characteristics is estimated.

2

Tyre Fundamentals

2.1 The Pneumatic Tyre

Tyres are highly engineered structural composites that can consist of more than 20 components and more than 15 rubber compounds [12]. During the manufacturing processes, the pneumatic tyres can be designed to meet certain criteria regarding handling and traction. The tyres are often highly overlooked by consumers, even though they are the only interface between the road and the vehicle, and play an important role when it comes to tyre-road friction [12].

2.1.1 Components

Compounds

The rubber compounds mainly consist of five different types of material ingredients: polymers, fillers, softeners, antidegradents and curatives [12]. Polymers are considered to be the basis of the rubber compounds, since they make up for the major proportion of the overall compound, and usually consist of synthetic or natural rubber. The prime function for the fillers are to reinforce the compound, and the commonly used filler in the industry is carbon black [12]. Softeners are used to help improving stickiness of the compound before it has been vulcanized, and examples of softeners are resins and waxes.

Antidegradents are used as protection against degradation by, for example, oxygen, heat and ozone [12]. Commonly used antidegradents are antioxidants, antiozonants and different waxes. Curatives are used during the vulcanization process, where the chains of the polymers get linked and transforms the rather viscous compound into a firm elastic material, and the most used material as a curative is sulphur [12].

Reinforcement Materials

Reinforcement materials are used primarily to strengthen and stabilize the tread and sidewall [12]. These materials are often synthetic materials such as polyester, aramid but can also be of other materials such as carbon steel. Worth noting is that all of these materials have their own set of advantages and disadvantages and plays a role for heat resistance, handling characteristics or even wear [12].

2.1.2 Tread and Pattern Design

The tread is essential for both the vehicle's traction and grip during driving, cornering and braking [12]. The tread compound is chosen to best yield a balanced performance when it comes to handling, traction and wear. The pattern of the tread is generally designed to provide a uniform wear and to yield a good performance in various driving conditions. There are numerous features of the tread pattern that directly affect traction, handling, noise and wear [12].

2.2 Tyre Mechanics

A coordinate system by the SAE standard, can be defined as in Figure 2.1 [7]. The figure also displays the forces and moments that act on the tyre. The longitudinal force F_x and the lateral force F_y are the forces that affects the vehicle handling and control [7]. These forces are typically generated in different situations. The tractive force F_x is generated when driving or braking and F_y is generated during cornering. Furthermore, the normal force F_z varies with the vehicle load.

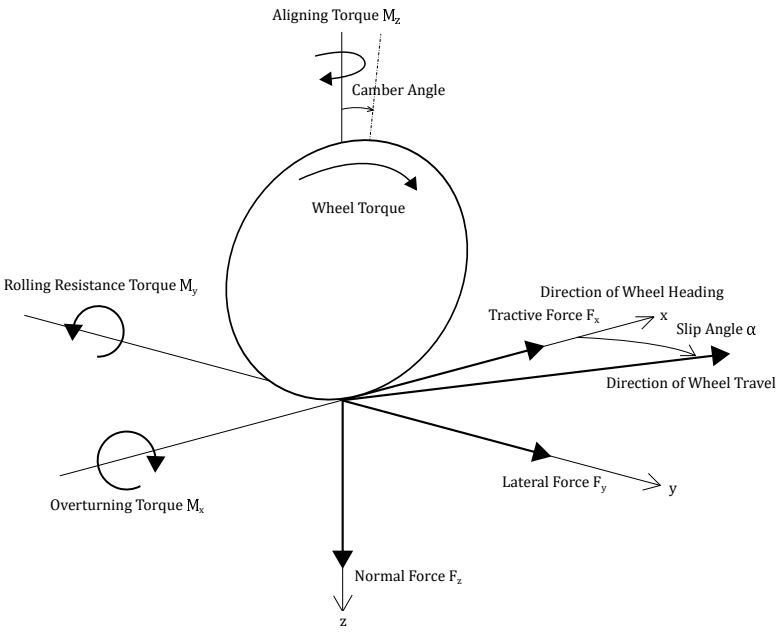

Figure 2.1: *The forces and moments acting on the tyre (SAE coordinate system), reproduced from [7].*

2.2.1 Longitudinal Slip

A wheel that is rolling freely, where no driving torque has been applied, over a flat surface and going in a straight line is considered to be an initial situation with a slip that is equal to zero by definition [13]. Due to rolling resistance, a force needs to be applied to overcome the resistance, and as a result a side force and self-aligning torque may be developed. The occurrence of a side force and self-aligning torque can be explained by the structure of the tyre not being completely symmetrical [13]. A deviating wheel motion from that of the initial situation, where the slip is equal to zero, results in wheel slip, additional deformations and possibly partial sliding in the contact patch between the tyre and the surface.

The longitudinal slip that appears when a driving torque is applied is defined as follows [13]:

$$\sigma_x = \frac{R_e\Omega - V_x}{V_x} \tag{2.1}$$

Here σ_x is the longitudinal slip, V_x the longitudinal component of the velocity vector of the centre of the wheel, R_e is the effective rolling radius and Ω is the angular velocity of the wheel. In the case of driving, the slip is positive, and the tractive force F_x is positive. During the case of braking, the slip is instead

negative. Furthermore, the effective wheel radius is defined as [13]:

$$R_e = \frac{V_x}{\Omega_0} \tag{2.2}$$

where Ω_0 is the freely rolling wheel's rotational speed.

2.2.2 Tractive Force

Under steady-state conditions, the developed tractive force F_x is proportional to the applied wheel torque, and the slip is therefore a function of the tractive force [14]. Initially the slip is a result of elastic deformations, and thus the tractive force and wheel torque increases linearly with slip [14]. As the longitudinal force and wheel torque increases, part of the tyre tread starts sliding, and the relationship between slip and tractive force stops being linear. From Figure 2.2, the linear relationship between the tractive force and longitudinal slip can be observed, and as the slip increases and the tyre tread starts sliding, the relationship becomes nonlinear.

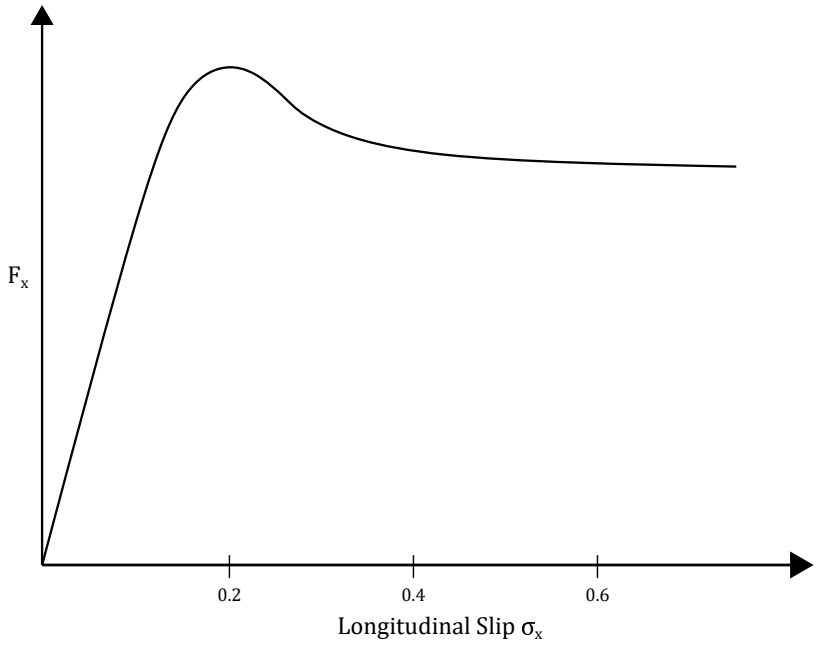

Figure 2.2: *Illustration of the relationship between the tractive force F_x and longitudinal slip σ_x.*

2.3 Tyre Wear

Wear is per definition material removal from a surface that is under the influence of frictional interaction with another surface [11]. The wear process of tyres is described to be a rather complex phenomena, since often times the amount of wear is measured/estimated after a long period of time, in which multiple processes other than sliding friction may have affected the wear process. These processes can, for example, be of mechanical, physical or chemical nature. Commonly considered mechanical wear mechanisms that affects tyre wear are adhesive wear and abrasive wear.

2.3.1 Adhesive Wear

Adhesive wear is one of the most fundamental types of wear, since this process takes place when two solid surfaces are in contact [15]. No matter how smooth the surfaces are, they will have contact at a few isolated points (see Figure 2.3).

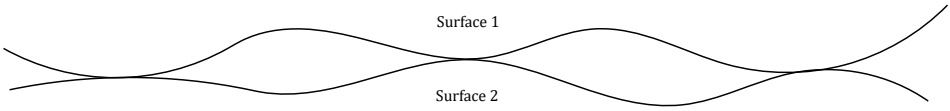

Figure 2.3: *Two surfaces in contact, where the isolated contact points are illustrated.*

The result of the adhesive process is that some of the material from the softer material transfers to the harder surface [15]. This can be explained by a high local pressure at the contact points combined with a sliding motion forming bonds at the contact points. Continuous sliding leads to the bonds being cut to the side of the softer material, thus resulting in material transferring from the softer surface to the harder.

The overall amount of material that is being transferred is primarily affected by the characteristics of the surfaces and the ambient conditions [15]. In regards of ambient conditions, a higher temperature results in a larger amount of adhesive wear. Since the bonds that are formed are on an atomic scale, and a higher temperature affects the rate of chemical reaction, the process of adhesive wear is accelerated [15]. The temperature is often times produced by the frictional heat that is being generated when two surfaces are rubbing against one and other.

2.3.2 Abrasive Wear

Abrasive wear is defined as the removal of solid material from a surface [15]. The removal of the material is a result of the material being gouged out by a harder surface. There exist two general cases for when abrasive wear occurs, in one case a softer surface is rubbing against a harder surface, and in the other case a third body, in many instances a particle of grit, is caught between two surfaces and the third body being harder than the other two surfaces. In the second case, the third body can either abrade one of the other surfaces or both at the same time.

2.3.3 Fatigue

Under rolling motion where two surfaces are in contact, indentations in the surfaces may occur as a result of fatigue due to repeated stresses under rotation [15]. For two surfaces under load, the distribution of elastic stresses in the material of each surface is in proximity to the contact area, and the maximum shear stress, force per unit area, occurs at a small finite distance beneath the surface [15]. Fatigue cracks generally start evolving close to where the maximum stress occurs, and once a crack has appeared, it propagates.

2.3.4 Aging Effects

Due to a variety of chemical reactions, detrimental changes occurs in the tyres properties after storage in ambient temperature or use on the vehicle during the period of five years [12]. One of the chemical reactions that occurs is between ozone and unsaturated elastomers that are being used in the compounds [12]. The reaction can lead to sharp cracks forming, and since ozone cannot directly penetrate the material, the reaction occurs at exposed surfaces. The forming cracks exposes more material for which ozone can react with, which in turn results in an increased number of cracks.

Another reaction process that causes aging effects is reaction with atmospheric oxygen (oxidation) [12]. This process is typically slower compared to the ozone reaction, but oxidation generally penetrates deeper. The result of oxidation is not directly cracks, but an increased hardness and brittleness of the material. The increased hardness of the material is caused by new crosslinks being formed, by hydrocarbon elastomers reacting with oxygen, and interacting with neighbouring molecules [12].

2.3.5 Conditions Affecting Tyre Wear

There are numerous different conditions that influence the overall tyre wear, ranging from different characteristics in road surfaces to the driving style itself.

Surface Influence

The characteristics of the road surface, in terms of its coarseness and sharpness, has a direct impact on tyre wear [12]. The structure of road surfaces may also vary depending on the season. Winter conditions typically yield a sharper road surface than in summer conditions, given moderate climates.

Construction Influence

A stiffer tyre construction generally produces a less amount of tyre wear, where the stiffer construction includes effects of tread pattern and stiffness in the tread compound [12].

Driving Influence

The driving style, characterized by the velocity and accelerations, have shown to have a significant impact on tread wear and the tyres' lifetime [12]. With an increasing vehicle velocity, the lifetime of the tyre is greatly reduced.

2.3.6 Vehicle Suspension

External factors such as vehicle suspension geometry has shown to have an influence of the wear [12]. Suspension dynamics primarily handles the motion and forces being produced during the tyre-road interaction [16]. Two common suspension settings are camber and toe alignment and will be further discussed below.

Camber

Camber is defined as the angle between the vertical of the tyre and the normal of the road surface (see Figure 2.4) [16]. The camber angle is positive if the tyre leans outwards from the body, and negative if it leans inwards. The general idea of having an inclination is that it provides another source of lateral force. In this case, where the lateral force comes from the inclination of a tyre, the lateral force is called a camber thrust [16]. The lateral force is essentially allowing the car to perform cornering manoeuvres and having a negative camber angle can help improving the cornering ability.

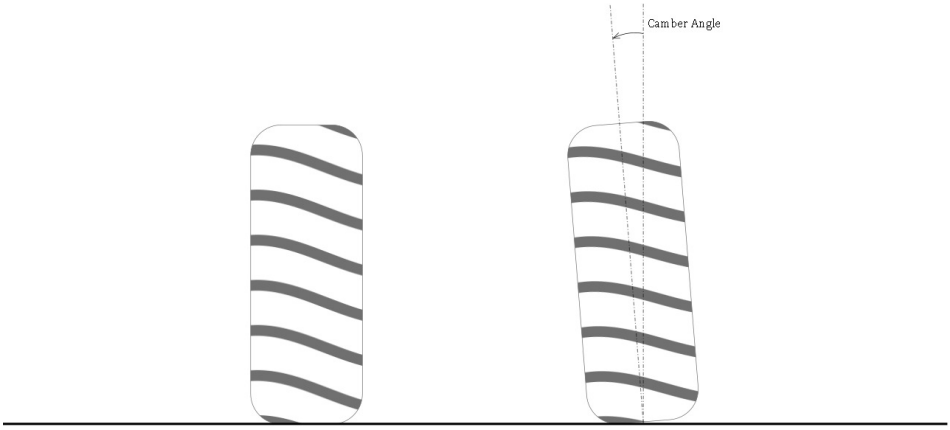

Figure 2.4: *A negative camber angle is illustrated.*

Toe

Toe alignment is defined as the angle between the tyres' longitudinal axis and the vehicle's axis (see Figure 2.5) [17]. If the toe alignment is such that the tyres are pointing inwards towards the vehicle's centre line, the alignment is generally called toe-in, and in the opposite case where they instead point outwards, it is labelled as toe-out. A bad tyre alignment can cause irregular wear and decrease the life-length of the tyres [12, 17].

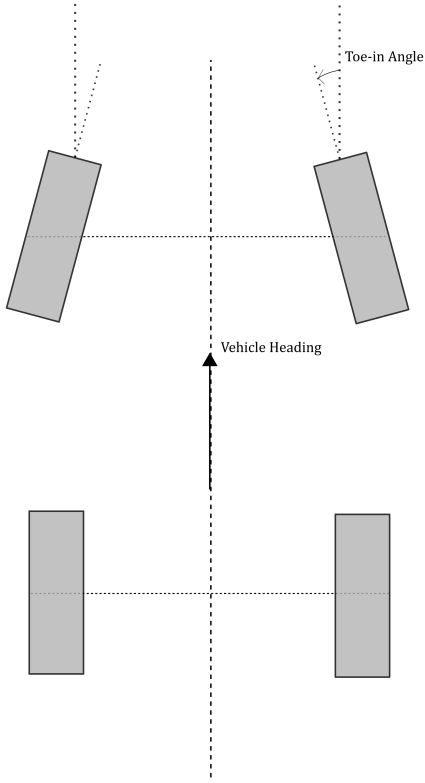

Figure 2.5: *Illustration of a toe-in angle.*

3

Friction Performance

One performance that is to be estimated is the friction performance. It has been shown in studies that the friction performance, the tyre grip on the road, in some cases has been more important for accident avoidance than driving with an electronic stability system (ESC) [18]. Furthermore, a higher vehicle velocity combined with a lower tyre-road friction yields a higher braking distance [19]. Moreover, active safety systems such as the anti-lock braking system (ABS) and ESC rely on their ability to control the vehicle's state of motion by application of induced tyre-road forces. These systems are therefore relying on the available tyre-road friction potential.

Since the tyre grip in winter conditions is critical for the avoidance of tyre-related accidents, the friction performance in the case of winter conditions is primarily studied.

3.1 Friction Potential

The total normalized traction force for a tyre can be expressed as follows [20]

$$\rho = \sqrt{\frac{F_x^2 + F_y^2}{F_z^2}} \tag{3.1}$$

Only considering the longitudinal direction, the normalized traction force (3.1) can instead be simplified to

$$\rho_x = \frac{F_x}{F_z} \tag{3.2}$$

Given ρ_x as a function of slip σ_x, $\rho_x(\sigma_x)$, a similar relationship as can be seen in Figure 2.2 occurs. Here the friction potential, the maximum tyre-road friction coefficient, is defined as

$$\mu_{x,max} = \max_{\sigma_x} \rho_x(\sigma_x) \tag{3.3}$$

Furthermore, Equation 3.3 defines the maximum normalized longitudinal force that can be generated in the contact patch of the tyre. In this thesis two friction regions are defined, where a low friction region is the friction potential in the interval $\mu_{x,max} < 0.45$, and a high friction region $\mu_{x,max} > 0.8$.

3.2 Tyre Stiffness

The longitudinal stiffness of the tyre, along with the friction potential, is considered to be one of the most important parameters and is defined as [10, 14]

$$C_x = \left.\frac{\partial F_x}{\partial \sigma_x}\right|_{\sigma_x=0} \tag{3.4}$$

Given the slip-force relation (Figure 2.2), the stiffness (3.4) is defined as the slope in the linear region. The slope can be seen as a limitation of the longitudinal force that can be generated, thus restricting possible vehicle motion [10]. Both the stiffness and friction potential will change depending on factors such as the road surface, wear, tyre temperature, and tyre properties in regard to constructional aspects.

3.3 Approach

By validating a Brush-model via experiments, it was implied that a relation between tyre stiffness and friction potential might be of a plausible existence [7]. Given these conclusions, it is in this thesis assumed that the stiffness correlates with the friction performance. If this proves to be accurate, and there is an unambiguous trend between the tyre stiffness and the tyres' friction potential, it is possible to express a model based on the trend. Given such a model, it would be feasible to predict the tyres' friction performance utilizing an estimated tyre stiffness as an input to the model.

3.3.1 Compensated Tyre Stiffness

Since the stiffness parameter is varying depending on various conditions such as the road surface and tyre temperature, it would be of a high difficulty to collect a large amount of data for different tyres, whilst having similar conditions, required for the purpose of observing correlations. By utilizing an estimated longitudinal tyre stiffness parameter from TGI, data collected at different occasions and locations, can be used to study the existence of a relation between stiffness and friction potential. The longitudinal tyre stiffness parameter from TGI is essentially an estimated tyre stiffness parameter (3.4) for a tyre driven in the high

friction region, that has been temperature compensated to an expected stiffness at a reference temperature through a compensation model. In this case the reference temperature is 20°C, and the compensated tyre stiffness is further denoted as C_{xr} in the thesis.

3.3.2 Trend Analysis

To study the existence of a correlation between the tyre stiffness and the friction potential in winter conditions, prior acquired data in the database is used. Utilizing TGI, estimates of the friction potential are available from logged CAN data and the friction estimates during ABS-braking in particular are used. Maximum longitudinal forces are, however, generated for large accelerations (forward) as well, but since this thesis is focusing on safety aspects, it is relevant to consider the case of braking. During ABS-braking the ABS-system might not in reality be able to hold the slip-force relation (Figure 2.2) around the peak, and estimated points are often altering between values on each side of the peak. The estimates of the friction potential used in this analysis are therefore similar to, but not necessarily identical to the peak value of the slip-force curve.

Furthermore, the entire database is used to create a table with a compensated stiffness parameter for each individual set of tyres. It can also be assumed that each test was conducted using vehicles of roughly the same dimensions, as a significant difference of dimensions could affect the vehicle's load drastically and thus yield a compensated tyre stiffness parameter that would appear rather misleading in the analysis.

4

Tread Wear Modeling

In order to estimate the tyre wear, a model needs to be implemented. In this thesis, only mechanical wear is considered, and tyre wear will thus further be referred to as tread wear. Given a tread wear model, effects of different ambient temperatures on tread wear for different types of tyres is to be studied.

4.1 Wear Models

There exist various tread wear models, mostly focusing on abrasive wear, and the models vary in complexity. More complex models tend to rely heavily on experimental data connected to tyre properties or road surface characteristics.

4.1.1 Empirical Wear Model

An extensive tread wear model, which has shown to produce good results in terms of usage for analysing the influence of different factors in various conditions, is proposed in research literature as follows [21]:

The abrasive and fatigue wear of a tyre:

$$I_a = \frac{3C_1}{C_2\zeta}\left[C_2\mu\frac{p}{p_0}\left(\frac{\zeta}{p}\right)^{1-\beta t}\right]^t p\frac{\sigma_x}{l} \tag{4.1}$$

where I_a is the wear quantity, ζ is a module of elasticity of the rubber material; C_1, C_2, βt — parameters regarding surface roughness; μ is the friction coefficient; t, p_0 are parameters concerning the fatigue curve of the rubber material; p is a nominal pressure on the surface; l the length of the contact patch and σ_x the

slip in the contact patch. By expressing $\left[C_2\mu\frac{p}{p_0}\left(\frac{\zeta}{p}\right)^{1-\beta t}\right]^t$ in Equation 4.1, that concerns surface and tyre material properties, as a coefficient k, Equation 4.1 now becomes [21]

$$I_a = \left(3C_1 p\frac{\sigma_x}{C_2\zeta l}\right)k = A_a p\frac{\sigma_x}{l} \tag{4.2}$$

where $A_a = \frac{3C_1}{C_2\zeta}k$. Equation 4.2 in a differential form can be expressed as [21]

$$I_a = A_a p\frac{d\sigma_x}{dl} \tag{4.3}$$

It is also proposed that the wear generated by side-slip α is proportional to the normal load and side-slip [21]. This wear can be expressed analogically to Equation 4.3 as

$$I_\delta = A_\delta p\frac{d\alpha}{dl} \tag{4.4}$$

where A_δ is a proportional coefficient analogue to A_a in Equation 4.3. The total wear is now given by

$$I = I_a + I_\delta \tag{4.5}$$

4.1.2 Archard's Wear Model

A physical model for expressing abrasive wear is Archard's wear model. This is a far more rudimentary model compared to the empirical model expressed in Chapter 4.1.1, and can be expressed as [22]

$$I = \xi\frac{F_z s}{H} \tag{4.6}$$

where I is the wear quantity; F_z is the vehicle load; s is a parameter for the sliding distance; ξ is a wear constant and H is the hardness of the rubber material. Furthermore, the term $F_z s$ can be approximated as the work done by friction in the longitudinal and lateral direction [22]

$$F_z s = W_x + W_y \tag{4.7}$$

Equation 4.6 can thus be approximated as

$$I = \xi\frac{W_x + W_y}{H} \tag{4.8}$$

4.1.3 Schallamach's Wear Model

Another simple abrasive wear model is Schallamach's wear model, albeit rudimentary, it has shown promising results that agrees with experimental data [23]. The wear quantity can be expressed as

$$I = \gamma F_z s \tag{4.9}$$

where γ is the abradability constant (abrasion per unit energy dissipation) and is expressed in the SI-unit mm^3J^{-1} [12, 23]. Approximating $F_z s$ as in Equation 4.7, Equation 4.9 can now be approximated by

$$I = \gamma(W_x + W_y) \tag{4.10}$$

Moreover, since γ is a constant

$$I \propto (W_x + W_y) \tag{4.11}$$

4.1.4 Choice of Model

Since no empirical data concerning tyre properties or the road surface is available, the two physical models are considered. Archard's wear model does, however, contain a parameter concerning the hardness of the rubber material, thus Schallamach's wear model (4.10) is the only feasible option with the least amount of unknown parameters.

4.2 Energy Rates

Given the law of energy conservation, the energy rates (power) in the longitudinal and lateral direction can be approximated as [24]

$$w_x = F_x V_{sx} \tag{4.12a}$$
$$w_y = F_y V_{sy} \tag{4.12b}$$
$$w = w_x + w_y \tag{4.12c}$$

where V_{sx} is the longitudinal slip velocity and V_{sy} is the lateral slip velocity. The slip velocity V_{sx} is defined as [13, 24]

$$V_{sx} = V_x - R_e\Omega \tag{4.13}$$

and the slip equation (2.1) can now be expressed as

$$\sigma_x = -\frac{V_x - R_e\Omega}{V_x} = -\frac{V_{sx}}{V_x} \tag{4.14}$$

so that

$$V_{sx} = -V_x\sigma_x \tag{4.15}$$

In the lateral direction the lateral slip velocity can be defined as $V_{sy} = V_y$, where V_y is the wheel-travel velocity in the lateral direction [24]. Furthermore, the total wheel-travel velocity $\sqrt{V_x^2 + V_y^2}$ deviates from the wheel orientation by the angle α (side slip angle) [7]

$$\tan\alpha = \frac{V_y}{V_x} \tag{4.16}$$

Under the assumption of small angles, Equation 4.16 yield

$$\alpha \approx \frac{V_y}{V_x} \tag{4.17}$$

and the lateral slip velocity can be expressed as

$$V_{sy} = V_x \alpha \tag{4.18}$$

The energy rates can now be approximated as

$$w_x = F_x V_x \sigma_x \tag{4.19a}$$
$$w_y = F_y V_x \alpha \tag{4.19b}$$

The sign in (4.19a) is neglected since a positive energy rate independent of direction is assumed.

4.3 Vehicle Dynamics

Given the equations for approximating the energy rates (4.19), the forces and longitudinal velocity needs to be estimated.

4.3.1 Force Estimation

It is assumed that the contact patch of a tyre can be divided into two different regions, where the regions are denoted as a sliding region and an adhesive region [14]. In the sliding region, the forces are depending on adhesive properties of the tyre-road interaction, whereas in the adhesive region the forces instead depend on elastic properties of the tyre. The total force acting on the contact patch is a sum of the force interacting in the sliding region and the force in the adhesive region [7, 14]. In the longitudinal direction we have

$$F_x = F_{sx} + F_{ax} \tag{4.20}$$

and in the lateral direction

$$F_y = F_{sy} + F_{ay} \tag{4.21}$$

Not utilizing a tyre model, such as the Brush-model, it is not possible to model the forces acting on the contact patch by the adhesive and sliding component explicitly. Utilizing the information from the automotive grade sensors, a single-track vehicle model can instead be used to approximate the total longitudinal and lateral forces acting on the front and rear axis.

Single-track Model

The single-track model, also commonly labelled as the bicycle model, is frequently used for studying planar vehicle motion. The model is illustrated in Figure 4.1.

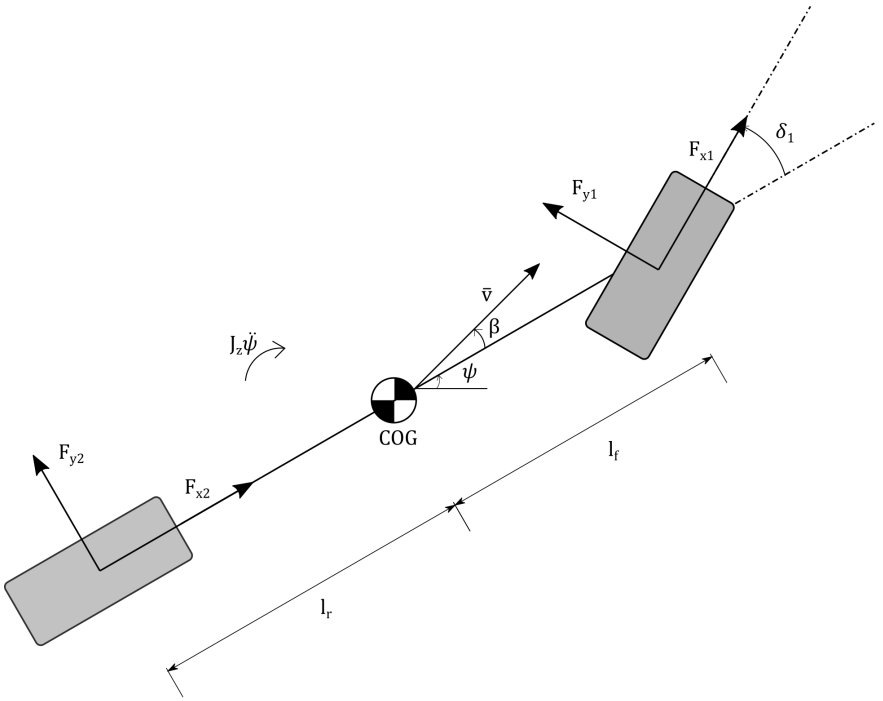

Figure 4.1: *Illustration of the single-track model.*

Fixating a coordinate system in the vehicle's body, Newtonian mechanics can directly be applied to obtain equations of motion. Equilibrium of the forces in the longitudinal and lateral direction, and moment equilibrium about the centre of gravity (COG) result in the following equations [25]

$$ma_y \sin\beta - m\dot{v}\cos\beta + F_{x2} + F_{x1}\cos\delta_1 - F_{y1}\sin\delta_1 = 0 \tag{4.22a}$$

$$ma_y \cos\beta + m\dot{v}\sin\beta - F_{y2} - F_{x1}\sin\delta_1 - F_{y1}\cos\delta_1 = 0 \tag{4.22b}$$

$$J_z\ddot{\psi} - l_f(F_{y1}\cos\delta_1 + F_{x1}\sin\delta_1) + l_r F_{y2} = 0 \tag{4.22c}$$

where m is the vehicle's mass; a_x and a_y is the longitudinal and lateral acceleration; β the body side-slip angle; $\dot{v}$ is the tangential acceleration, which is directed tangentially to the trajectory; F_{xi} and F_{yi}, $i = 1, 2$, are the forces acting on the rear and front axle in each direction; δ_1 is the steering angle; J_z is the moment of inertia about COG; l_f and l_r are the distance from the front and rear axles to COG respectively and $\ddot{\psi}$ is the yaw-acceleration. The equations of motion expressed in (4.22) have been simplified to not consider drag forces.

Further simplifications, such as, assuming that $\beta = 0$, we now have the following set of equations

$$ma_x = F_{x2} + F_{x1}\cos\delta_1 - F_{y1}\sin\delta_1 \tag{4.23a}$$

$$ma_y = F_{y2} + F_{x1}\sin\delta_1 + F_{y1}\cos\delta_1 \tag{4.23b}$$

$$J_z\ddot{\psi} = l_f(F_{y1}\cos\delta_1 + F_{x1}\sin\delta_1) - l_r F_{y2} \tag{4.23c}$$

4.3.2 Velocity

It is possible to obtain a vehicle velocity from Global Positioning System (GPS) equipment, but this source cannot be entirely relied on. Not every vehicle is equipped with GPS equipment, and in rather occluded areas a stable signal from the satellites might not be of existence. A far more reliable source are the wheel speed sensors that are used in the ABS-system. Given a rotational velocity from the wheel speed sensors and tyre dimensions, a longitudinal velocity can be approximated for each tyre.

Before translating the tyre velocities into a vehicle velocity V_x, some precautions need to be made. In the case of a sharp cornering manoeuvre on a high friction surface, load on the inner tyres is drastically decreased and might cause the driven inner tyre to spin if additional accelerations are applied when exiting the turn. This scenario can be recognized by looking at the difference in wheel speed of a non-driven and driven tyre on the same side of the vehicle. If the difference is above a certain threshold for normal situations, these values should be neglected when approximating the longitudinal vehicle velocity.

4.4 Simplified Wear Model

In this thesis, the side-slip angle α, will not be considered when modelling tread wear, as this makes the modelling procedure far more complex. Moreover, taking lateral dynamics into consideration would also make the results more difficult to analyse since it would be difficult to study the impact on tread wear each direction has. The complete tread wear model can now, under the assumption of $\alpha = 0$, be expressed as follows

$$I = \gamma W_x \tag{4.24}$$

which is proportional to the friction work in the longitudinal direction ($I \propto W_x$). Furthermore, the power rate w_x can be integrated over time to approximate the total work W_x

$$W_x = \int_0^{t_f} w_x \, dt \tag{4.25}$$

where t_f is the total travel time. We now have the following equation to express the tread wear over time

$$I = \gamma \int_0^{t_f} F_x V_x \sigma_x \, dt \tag{4.26}$$

4.5 Simulation of Temperature Effects

A model for estimating tread wear over time is proposed in (4.26), that only utilizes available information from the automotive grade sensors. The wear model is therefore feasible to implement in an online setting for wear approximation. The abradability constant γ in the wear model (4.26) remains, however, an unknown parameter and is assumed to be highly tyre specific. The direct consequence of this is that the information from the wear model cannot be used to evaluate if the tyres that are currently being used are under the effect of a higher wear, since it is not possible to accurately compare different tyres, i.e., compare the wear to a reference.

In order to omit the parameter in this study, the relative change in tread wear for a specific tyre is instead considered. More specifically, the relative change in wear for different ambient temperatures is examined. It is relatively well known that, for example, soft winter tyres should not be used in a higher temperature since the tread wear is considered to be higher [26]. It is therefore further investigated if the defined wear model (4.26) can capture the effect of softer tyres being more affected by ambient temperature in regards of an increased wear.

Given the tyre stiffness C_x (3.4) and the assumption of low amounts of excitation, such that $\rho_x(\sigma_x) = C_x \sigma_x$, a way of approximating slip based on the tyre stiffness parameter is as follows

$$\sigma_x = \frac{\rho_x}{C_x} \tag{4.27}$$

where ρ_x is the normalized traction force (3.2). To study if the wear model can describe the phenomena of certain tyres being more likely to wear faster for higher ambient temperatures, the fact that the tyre stiffness parameter C_x changes with tyre temperature is utilized. A softer tyre will have a stiffness parameter that is far lower than for stiffer tyres, which would yield a larger slip according to the slip equation (4.27). A larger slip value would result in a higher energy rate w_x, thus presumably increasing the tyre temperature, which would modify the stiffness parameter further.

4.5.1 Simulation Environment

A simulation is set up such that an energy rate w_x is estimated given the inputs V_x, ρ_x, F_z, C_x. This estimated energy rate is acting as an input to a temperature model implemented by NIRA that estimates a tyre temperature having the energy rate w_x, V_x and ambient temperature T_{amb} as an input. The output, a new tyre temperature T_{tyre}, is an input for a compensation model, also developed by NIRA, that takes a stiffness parameter in reference temperature C_{xr}, described in Chapter 3.3.1, and compensates it to an expected stiffness given a tyre temperature. The output from the compensation model is a stiffness parameter C_x which is then used to calculate a new energy rate.

A flowchart of the simulation environment is illustrated in Figure 4.2. It is now possible to investigate how different values of C_{xr} is affecting the energy rate, thus possibly affecting the tyre temperature, which in turn modifies C_x more. A significant increase of energy rate would yield a higher wear given the wear model (4.24). The inputs V_x, ρ_x, F_z, C_{xr} and T_{amb} are here assumed to be known and used to simulate an arbitrary driving situation, such as driving forward in a straight line with a constant velocity with a fix ambient temperature.

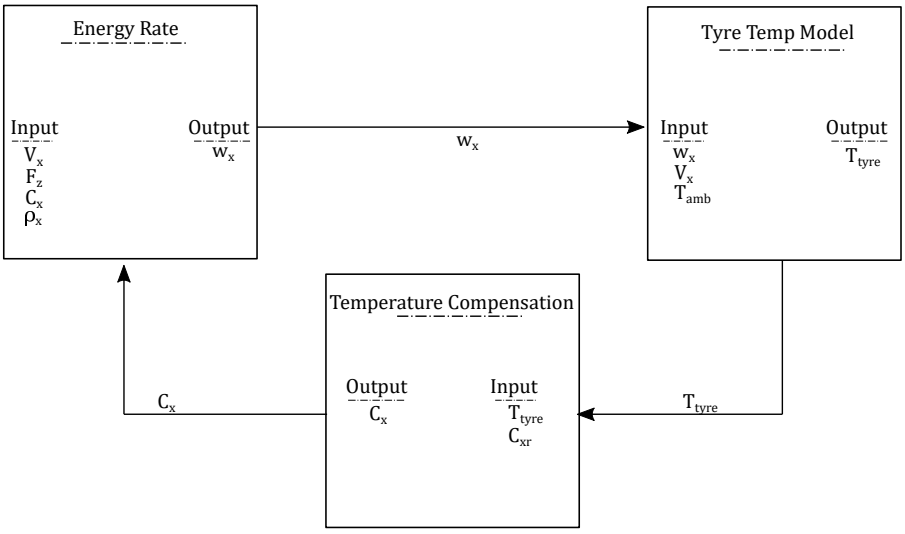

Figure 4.2: *A flowchart of the simulation environment.*

4.5.2 Expected Wear

Given an estimated tyre stiffness parameter C_{xr}, the temperature model, and the temperature compensation model described in Chapter 4.5.1, it is feasible to approximate an expected wear for different temperatures in an online setting using the slip approximation in (4.27). If the wear model captures the effects of the phenomena discussed in Chapter 4.5, a relative change in wear can be expressed as

$$I_{rel} = \frac{I_{est}}{I_{ref}} \tag{4.28}$$

where I_{ref} is the wear under the current conditions and I_{est} is the expected wear for a given temperature. The estimated wear difference I_{rel} could then be used to predict if the tyres would be a subject to an unexpectedly high amount of wear caused by a higher ambient temperature.

5

Velocity Performance

When looking at safety aspects, one important performance indicator to consider is the velocity performance of the tyres. High velocities and friction can, for example, lead to higher forces, which could affect the tyres' ability to steer and control the vehicle. In literature, there is a concept of tyre-force ellipses which demonstrates limiting forces [27]. If the magnitude of the resultant force of the lateral and longitudinal force is within this ellipse, then the ability for the tyres to control the vehicle is maintained.

The velocity performance is in this thesis, however, defined as a critical vehicle velocity V_{max}, which is a maximum velocity for which the driver still can perform cornering manoeuvres correctly without losing the path around the corner. If the velocity is increased beyond this limit, the path around the corner is lost.

5.1 Lateral Dynamics

Cornering manoeuvres are assumed to be crucially dependent on lateral dynamics and therefore dependent on the lateral force generated in the contact patches. When the vehicle is cornering, the lateral force on the rear and front tyres generates a moment equilibrium about COG and counteracts the centripetal force [16]

$$F_c = \frac{mV^2}{r} \tag{5.1}$$

where r is the corner radius.

5.1.1 High Velocity Cornering

In the case of a high velocity corner, the COG has moved further to the rear axle compared to when it was in the geometrical centre [16]. Again, considering the single-track model (Figure 4.1) and the forces acting on the front and rear contact patch, the following equation is required to be fulfilled for the vehicle to be in moment equilibrium about COG [16]

$$F_{y2} l_r = F_{y1} l_f \tag{5.2}$$

If the COG is further back closer to the rear axle, such that $l_f > l_r$, it directly follows that $F_{y2} > F_{y1}$ and thus consequently $\alpha_2 > \alpha_1$, where α_2 is the side-slip for the rear tyre and α_1 the side-slip for the front tyre. If a high enough velocity V_{max} is obtained, such that the forces generated are nearing the nonlinear region given the force-slip relation, not enough force might be generated in the rear contact patch such that equilibrium is achieved. The direct consequence is that the vehicle is not able to maintain the path around the corner.

5.1.2 Lateral Friction Potential

Analogically to that of the normalized traction force in the longitudinal case (3.2), a normalized lateral traction force ρ_y can be derived from (3.1). If only lateral dynamics are considered, the normalized lateral force is defined as [20]

$$\rho_y = \frac{F_y}{F_z} \tag{5.3}$$

Given ρ_y as a function of the side-slip angle α, the available lateral friction potential is defined as

$$\mu_{y,max} = \max_{\alpha} \rho_y(\alpha) \tag{5.4}$$

Similarly to (3.3), the lateral friction potential (5.4) defines the maximum lateral force that can be generated in the contact patch.

5.1.3 Lateral Stiffness

The lateral stiffness is defined analogically to (3.4) as [7, 14]

$$C_y = \left. \frac{\partial F_y}{\partial \alpha} \right|_{\alpha=0} \tag{5.5}$$

Again, approximated as the slope in the linear region of the force-slip relation. Both the lateral stiffness and the lateral friction potential are dependent on similar external factors described in Chapter 3.2. The slope, lateral stiffness, acts as a limitation of the amount of lateral force that can be generated in the contact patch.

5.2 Approach

A reasonable approach would be to approximate the lateral stiffness parameter (5.5) and the lateral friction potential (5.4), and estimate V_{max} in a more analytical manner. This approach is, however, assumed to be highly difficult, especially in an online setting. A, perhaps, more intuitive approach is considered, which is based on conducting experiments and analysing trends similarly to the approach described in Chapter 3.3. It is further investigated if there is a correlation between a critical velocity V_{max} and an estimated longitudinal stiffness parameter C_{xr}, where V_{max} is determined by experiments. Analogically to the approach discussed in Chapter 3.3, if there is an unambiguous trend, a model could be implemented based on the given trend. Having a compensated longitudinal stiffness parameter C_{xr}, the critical velocity could then be predicted.

5.3 Data Acquisition

To determine the critical velocity V_{max}, a double lane change test (ISO 3888-2) is performed [28]. This test was chosen mainly because of the fact that the rather uncomplex experimental setup allows for an adequate reproducibility of results, but also since it is a well-tested method. The experimental setup is illustrated in Figure 5.1.

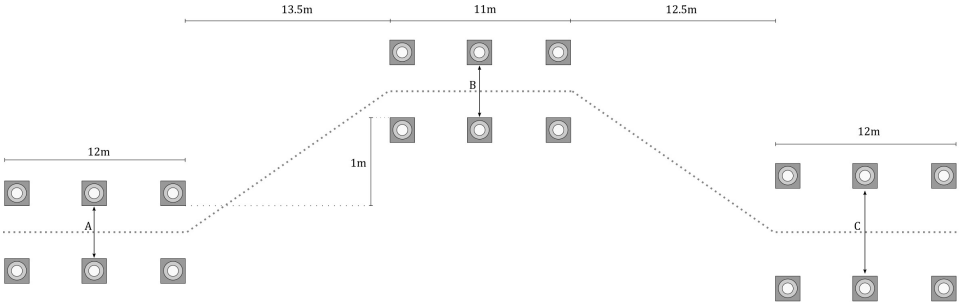

Figure 5.1: *Illustration of the double lane change experimental setup, reproduced from [28].*

The three lanes are defined with cones and the main goal is for the driver to perform the two lane change manoeuvres without knocking down any of the cones. The driver accelerates the vehicle to a specific velocity and keeps it constant, and upon entering the first lane (marked A in Figure 5.1) the throttle is released. The width of the first and second lane (A and B) are both dependent on the width of the vehicle, and the width of the exit lane C is 3 m. The test is performed for various velocities until the critical velocity V_{max} is determined, which is set when any of the cones are overturned.

6
Results

In this chapter the results are presented. For the friction performance and velocity performance, the trend analysis discussed in Chapter 3.3.2 and results from the executed experiment described in Chapter 5.3 are presented. The proposed tread wear model in (4.26) is evaluated by its ability to predict if softer tyres would be prone to have a higher amount of tread wear in a higher ambient temperature. At the request of NIRA, the x-axis in Figure (6.1, 6.2) and the y-axis in Figure (6.4, 6.5, 6.6) has been removed.

6.1 Friction Performance

Data from 26 different tests with unique tyre sets, where the tests were carried out in winter conditions, is used to perform the trend analysis as described in Chapter 3.3.2. In this case, all of the tyres were driven on snow-covered road surfaces. The result of plotting the estimates of friction potential from the different data collections against the corresponding stiffness parameter for each tyre is presented in Figure 6.1. To further emphasize the existence of a trend, the friction potential is plotted against the inverse value of C_{xr}. As expected, the friction performance is considerably higher for winter tyres compared to summer tyres when driving on snow. It is also quite evident that there is a tendency for a trend where softer tyres (increasing C_{xr}^{-1}) tend to perform better.

Furthermore, two winter tyres are substantially stiffer than the other winter tyres and performs just as bad as the summer tyres. As it turns out, both of these tyres had passed their lifetime of five years, and as described in Chapter 2.3.4, detrimental aging effects occurs over time. This could be the very reason they are substantially stiffer compared to the other winter tyres and thus presumably the reason why they are showcasing a poor friction performance.

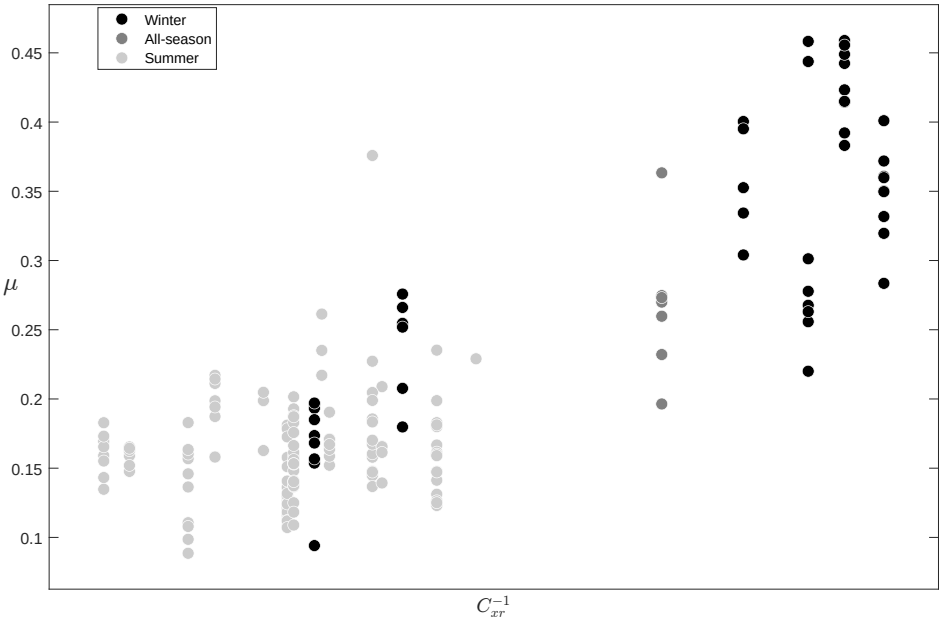

Figure 6.1: *Estimates of friction potential from individual tests are plotted as a column vector against corresponding* C_{xr}^{-1}.

To further investigate the existence of a trend, a simple linear regression model on the form $y = X\beta = \beta_0 + \beta_1 x$ is implemented. The model is fitted to the mean of estimated friction potentials for each tyre set in Figure 6.1, and is presented with both the 3σ and 95% confidence intervals in Figure 6.2.

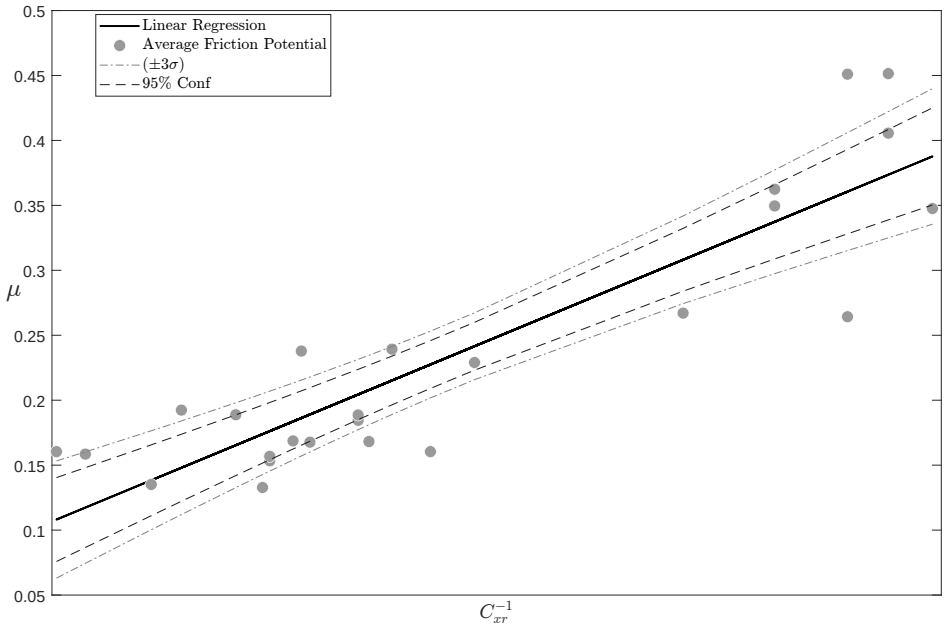

Figure 6.2: *An estimated linear regression model, fitted to the mean of estimated friction potentials for each tyre set, is presented with the* 3σ *and* 95% *confidence intervals.*

The coefficient of determination, evaluated as $R^2 = 1 - \dfrac{\sum_i (y_i - \hat{y}_i)^2}{\sum_i (y_i - \bar{y})^2}$, where y is the observed data; $\hat{y}$ are the expected values stemming from the regression model and $\bar{y}$ is the mean of the observed data, yield a model fit of approximately 80%. A model fit of 80% implies that there are tendencies for a linear trend, but the proposed linear regression model in Figure 6.2 is far from perfect.

The residual $\epsilon_i = y_i - \hat{y}_i$ plotted against the fitted values $\hat{y}$ is presented in Figure 6.3.

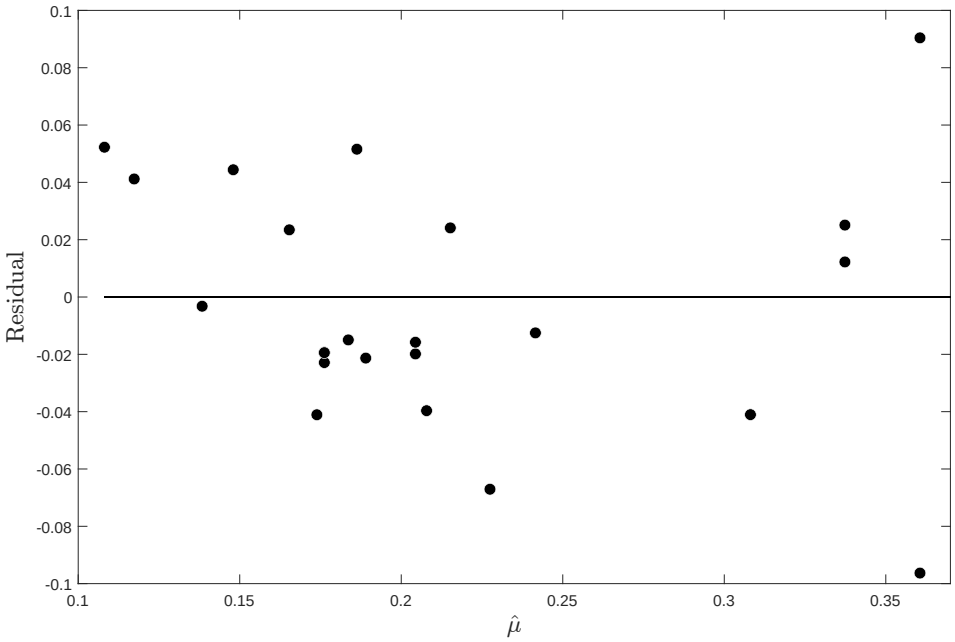

Figure 6.3: *The residual plotted against the fitted values.*

The errors does not seem to follow a specific pattern, which implies that the model is correct on average rather than systematically estimating too low or high values.

6.2 Tread Wear

The simulation environment described in Chapter 4.5.1 is utilized to evaluate the wear model (4.26) by its ability to capture the effects of different tyres, in terms of stiffness, having a larger amount of tread wear in higher ambient temperatures. In this simulation, only the front tyres are examined. An arbitrary and simple driving case is considered, where the vehicle is traveling at a constant velocity in a straight line, with both a constant traction force and normal force acting on the front tyres. The forces acting on the contact patches are here assumed to be equal on both of the front tyres. The parameters in the simulation environment are set according to Table 6.1.

V_x	100 [km/h]
F_z	4865 [N]
ρ_x	0.1 [−]

Table 6.1: *Parameter initialization for the simulation environment.*

The stiffness parameter C_{xr} and ambient temperature T_{amb} will vary to study the case of a softer and stiffer tyre in a lower and higher ambient temperature. A temperature of 7°C is here defined as a lower ambient temperature, since it is often considered to be a rule of thumb not to drive with softer tyres in $T_{amb} > 7$°C due to an expected higher wear rate. An ambient temperature of 40°C is chosen as a higher temperature in this analysis, which is a rather extreme case.

When comparing the energy rates in Figure 6.4, it is apparent that the softer tyre has a significantly larger energy rate compared to the stiffer tyre, which is to be expected given the slip equation (4.27). It is also clear that a higher ambient temperature yields a higher energy rate.

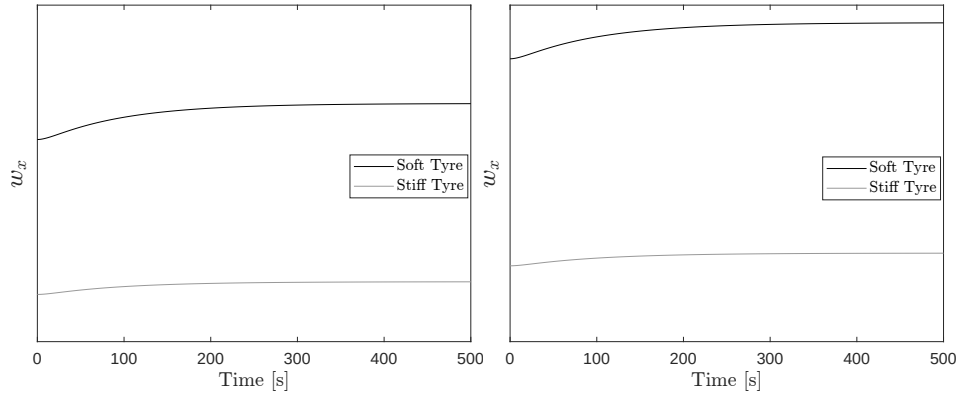

(a) *Energy rates in a low ambient temperature.*

(b) *Energy rates in a high ambient temperature.*

Figure 6.4: *Simulated energy rates for a low and high ambient temperature.*

The significant difference in energy rates between the softer and stiffer tyre does not seem to affect the tyre temperature substantially. In Figure 6.5 only a minuscule difference can be observed between the tyre temperature for a softer and stiffer tyre. The same result is observed for the tyre temperature for a higher ambient temperature (Figure 6.6).

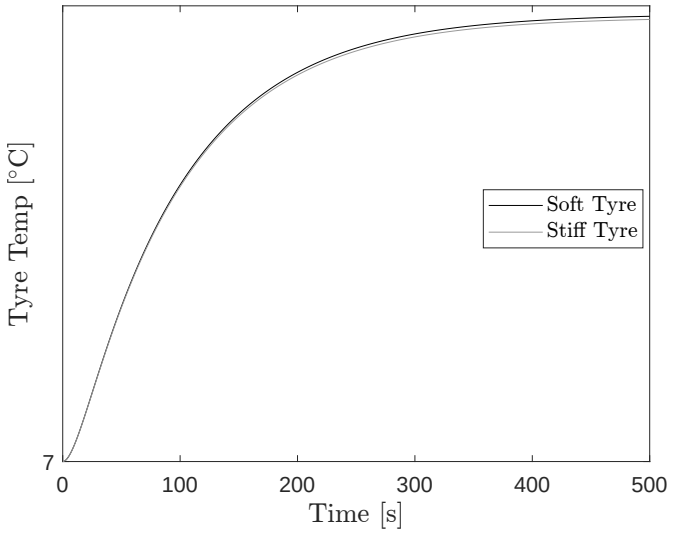

Figure 6.5: *Simulated tyre temperature for a low ambient temperature.*

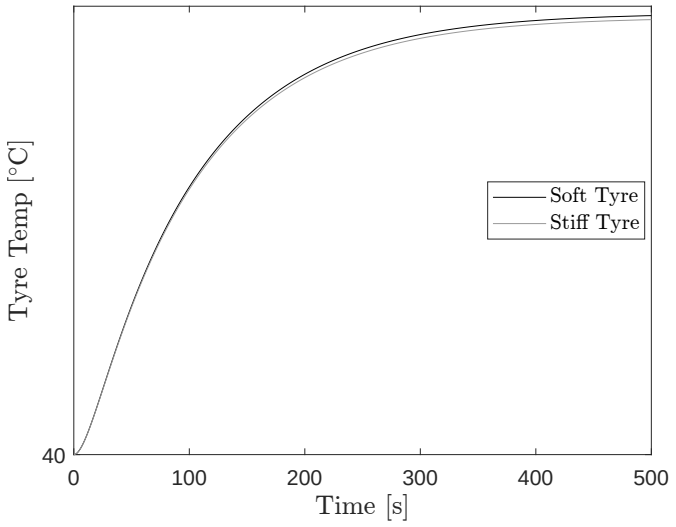

Figure 6.6: *Simulated tyre temperature for a high ambient temperature.*

Since the energy rates has such a small impact on the tyre temperature, it is not expected that the wear model (4.26) can describe the phenomena correctly. Given the fact that the tyre temperature modifies the stiffness further, and the tyre temperature is showing such a minuscule difference when comparing a stiff and soft tyre, the relative change in stiffness would not be drastically higher for the softer tyre compared to the stiffer tyre. Moreover, the wear model is implemented in the simulation environment to study the relative wear difference I_{rel} for a lower

and a higher ambient temperature. The relative wear difference is calculated as $I_{rel} = \left| \frac{I_{high} - I_{low}}{\max(I_{low}, I_{high})} \right|$. It is evident when studying the relative difference of tread wear in Figure 6.7, that the relative difference is higher for the stiffer tyre compared to the softer tyre, which is a direct result of the stiffness being modified more relatively by the temperature compensation model for the stiffer tyre compared to the softer tyre. This further indicates that the proposed wear model is rather inadequate in an online setting and cannot explain the phenomena fully.

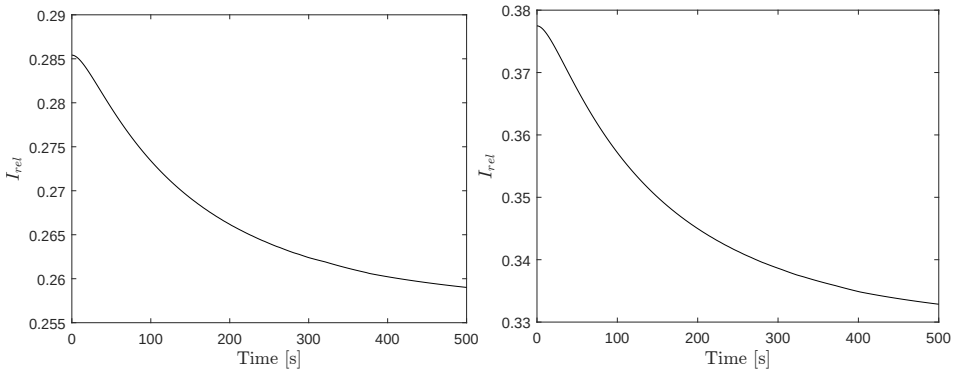

(a) *Relative wear difference I_{rel}, for a soft tyre, for a low and high ambient temperature.*

(b) *Relative wear difference I_{rel}, for a stiff tyre, for a low and high ambient temperature.*

Figure 6.7: *Relative wear difference for a low and high ambient temperature.*

6.3 Velocity Performance

The experiment described in Chapter 5.3 was executed by a professional driver, and the double lane change test was performed for two different sets of tyres of each type (winter, all-season and summer). The conditions were equal for all the tests that were performed, and the tests were performed on a high friction road surface (dry asphalt) for an ambient temperature $T_{amb} \in [5, 10]°C$. The driver systematically increased the velocity until V_{max} was determined, and for each velocity the lane change test was performed three times in order to minimize possible variances stemming from the driver. The results are presented in Table 6.2.

Type	C_{xr} [N]	V_{max} [km/h]
Winter (not studded)	29	70
Winter (not studded)	32	70
All-season	36	80
All-season	43	70
Summer	50	70
Summer	60	80

Table 6.2: *Results from the double lane change test (ISO 3888-2).*

The results are quite unexpected, as there are no substantial differences in V_{max} between the different types of tyres. The remarks given by the driver were that the tyre with the lowest C_{xr} value had the worst grip of all the tested tyres, and the grip got increasingly better as C_{xr} increased. This does, however, contradict the results as the softest tyre performed just as well as a stiffer summer tyre. For a tyre with a bad grip, it is expected that the critical velocity is smaller, since the forces that can be generated in the contact patches are much more limited.

6.4 Discussion

The linear regression model presented in Figure 6.2 could possibly be used in an online setting to roughly indicate the friction performance in winter conditions (snow-covered road surface) of the equipped tyres, given an estimated stiffness parameter C_{xr}. The precision of the expected value of the friction potential is, however, not considered to be high since the model fit is only 80%.

When evaluating the tread wear model, it is apparent from the results that the model is insufficient when it comes to its ability to be able to accurately indicate if the tyres are under the influence of a higher tread wear due to a higher ambient temperature. The energy rates have such a small impact on the tyre temperature, even though a softer tyre has a significantly larger energy rate compared to a stiffer tyre. The direct consequence is that it is not sufficient to use the wear model and calculate a relative wear difference in order to make a prediction. This indicates that another model, which has different sets of parameters to better describe the temperature phenomena, needs to be derived.

Abrasive wear has shown to increase with an increased temperature, and the increased wear under a higher temperature is believed to be a result of the oxidation process being accelerated by the temperature [29]. This implies that the oxidative process might need to be included in a model, for it to accurately describe the phenomena. Moreover, the proposed wear model in this thesis does not include any parameters describing the road surface such as the road roughness, and since ambient temperature affects the road surface by, for example, making it sharper if the ambient temperature is low, the tread wear model would not de-

scribe the wear effects caused by changes in the road surface. The empirical wear model defined in Chapter 4.1.1 does contain several parameters concerning the road surface, and is theoretically capable of describing these effects. Empirical wear models are, however, considered not to be a viable choice for online estimation, since it relies heavily on experimental data.

Lastly, it is evident from Table 6.2 that there are no significant differences in V_{max} for the tyres that were tested, and there is certainly no apparent correlation between C_{xr} and V_{max}, even though the difference in tyre-road grip was distinct according to the test driver. This raises the question if there is no correlation whatsoever between longitudinal stiffness and the critical velocity, or if the driver unknowingly made compensations in the manoeuvring for the tyres with a bad grip in order to execute the test without overturning any cones. The ISO 3888-2 test has to some extent been criticized for being highly dependent on the skills of the driver [28]. Therefore, it might just be that the influence the driver's skill had on the test has been severely underestimated when deciding on this approach.

A clear limitation for the conducted experiment in this thesis was the ambient temperature, which was fairly low for the test occasions. If the tests were to be conducted in more extreme temperatures, it is possible that some more distinct differences in V_{max} would appear for different types of tyres.

7

Conclusions

In this thesis, the feasibility of estimating three different performances (friction performance, tread wear, and velocity performance) for the tyres in an online setting has been investigated. Previous research of this area is rather limited, and the general problem of online estimation is the lack of information regarding specific tyre characteristics. Given this problem, only information available from the automotive grade sensors is used to investigate the possibility to derive rudimentary models for online usage.

It is concluded from the results that the proposed linear regression model could possibly be used in an online setting to roughly indicate the tyres friction performance in winter conditions (snow-covered road surface), given an estimated stiffness parameter C_{xr}. The results therefore imply that information available from the automotive grade sensors can be used to predict the tyres friction performance in winter conditions.

From the results concerning velocity performance, no usable information can be extracted, since it cannot directly be concluded that there is no correlation between C_{xr} and a critical velocity V_{max}. In order to obtain unbiased results, other methods need to be considered. No conclusions, whether information from the automotive grade sensors can be used to predict the tyres velocity performance or not, can therefore be made.

It is lastly concluded that the suggested wear model, that utilizes information from the automotive grade sensors, cannot be used in an online setting to indicate if the tyres are under the influence of a higher wear caused by a higher ambient temperature. Other models that can better describe the temperature phenomena need to be derived in order to accurately indicate a higher wear due to a higher

ambient temperature in an online setting.

7.1 Future Work

Estimation of tread wear in an online setting to indicate if the tyres are under the influence of a higher wear due to, for example, a higher ambient temperature as was investigated in this thesis, is a difficult problem to solve. Mainly because existing tread wear models are relying on parameters that are dependent on specific tyre characteristics, and in an online setting no such information is available. The research in wear estimation in an online setting is limited, and it would be interesting to see a continuation of this research area. Instead of using physical tread wear models, an alternative approach could be to investigate the feasibility to derive a wear model based on collected data, where the actual wear has been measured by either weighing the tyres or measuring the difference in tyre radius.

Regarding the velocity performance, it would be interesting to see if experiments that deduct the influence of a driver completely would yield different results, where a distinct difference in V_{max} is shown for different types of tyres. It would also be of interest to see if the conducted experiment in this thesis would yield significant differences in the critical velocity for different tyres if the tests were to be repeated in more extreme ambient temperatures. In order to estimate the velocity performance accurately in an online setting, an approach where the critical velocity is estimated analytically might, however, need to be investigated.

Bibliography

[1] Mattias Hjort and Håkan Andersson. Road safety effects associated with tires, rims and wheels. URL http://urn.kb.se/resolve?urn=urn:nbn:se:vti:diva-591. Accessed 2021-01-21.

[2] O. Bulan, E. A. Bernal, R. P. Loce, and W. Wu. Tire classification from still images and video. In *2012 15th International IEEE Conference on Intelligent Transportation Systems*, pages 485–490, 2012.

[3] Tetsuya Tanizaki, Koji Ueda, Toshihiko Murabe, Hideyuki Nomura, and Tomoo Kamakura. Identification of winter tires using vibration signals generated on the road surface. *Applied Acoustics*, 83:116 – 122, 2014.

[4] Johan Strandroth, Matteo Rizzi, Maria Ohlin, Jenny Eriksson, and Anders Lie. Analysis of different types of winter tyres in rear-end injury crashes and fatal loss-of-control crashes with esc. URL https://www.trafikverket.se/contentassets/af96c157fb7747a598cb2915bc5739b2/rapport.pdf. Accessed 2021-01-21.

[5] Beate Baensch-Baltruschat, Birgit Kocher, Friederike Stock, and Georg Reifferscheid. Tyre and road wear particles (trwp) - a review of generation, properties, emissions, human health risk, ecotoxicity, and fate in the environment. *Science of The Total Environment*, 733:137–823, 2020.

[6] Kaidi Zhang, Yupeng Duan, Xiaobo Yang, James Yang, and Yunqing Zhang. Determination of magic formula tyre model parameters using homotopy optimization approach. *SAE Technical Paper 2020-01-0763*, 2020.

[7] Jacob Svendenius. *Tire Modeling and Friction Estimation*. PhD thesis, Department of Automatic Control, Lund University, 2007.

[8] Wei Liang, Jure Medanic, and Roland Ruhl. Analytical dynamic tire model. *Vehicle System Dynamics*, 46(3):197–227, 2008.

[9] Iraj Davoodabadi, Ali Asghar Ramezani, Mehdi Mahmoodi-k, and Pouyan Ahmadizadeh. Identification of tire forces using dual unscented kalman filter algorithm. *Nonlinear Dynamics*, 78(3):1907–1919, 2014.

[10] Anton Albinsson. *Online and Offline Identification of Tyre Model Parameters*. PhD thesis, Department of Mechanics and Maritime Sciences, Chalmers University of Technology, 2018.

[11] V.H. Nguyen, D. Zheng, F. Schmerwitz, and P. Wriggers. An advanced abrasion model for tire wear. *Wear*, 396-397:75–85, 2018.

[12] A. N. Gent and J. D. Walter. Pneumatic tire. *Mechanical Engineering Faculty Research*, 854, 2006.

[13] H. B. Pacejka. *Tyre and Vehicle Dynamics*. Butterworth-Heinemann, 2nd edition, 2006.

[14] J. Y. Wong. *Theory of Ground Vehicles*. Wiley, 4th edition, 2008.

[15] John T. Burwell. Survey of possible wear mechanisms. *Wear*, 1(2):119–141, 1957.

[16] J. Balkwill. *Performance Vehicle Dynamics: Engineering and Applications*. Butterworth-Heinemann, 2018.

[17] Bridgestone Americas Tire Operations LLC. What you need to know about tire alignment. URL `https://www.bridgestonetire.com/tread-and-trend/drivers-ed/tire-alignment#`. Accessed 2021-04-09.

[18] Mattias Hjort. Measuring tyre performance in esc intervention situations. *Proceedings of the international conference Science meets Tires: Perspectives for Tire Technology. Aachen*, 2013.

[19] Yumrak Oh and Hoguen Lee. Characteristics of a tire friction and performances of a braking in a high speed driving. *Advances in Mechanical Engineering.*, 6, 2014.

[20] M. Doumiati, A. Charara, A. Victorino, and D. Lechner. *Vehicle Dynamics Estimation using Kalman Filtering: Experimental Validation*. John Wiley and Sons, Incorporated, 2012.

[21] Rosen Ivanov. Tire wear modeling. *Transport Problems*, 11(3):111–120, 2016.

[22] P. Flores. Modeling and simulation of wear in revolute clearance joints in multibody systems. *Mechanism and Machine Theory*, 44(6):1211–1222, 2009.

[23] A. Schallamach and D.M. Turner. The wear of slipping wheels. *Wear*, 3(1): 1–25, 1960.

[24] Bin Ma, Hong guo Xu, Yong Chen, and Mu yi Lin. Evaluating the tire wear quantity and differences based on vehicle and road coupling method. *Advances in Mechanical Engineering*, 9(5), 2017.

[25] Martin Meywerk. *Vehicle Dynamics*. John Wiley and Sons, Incorporated, 2015.

[26] Continental Reifen Deutschland GmbH. Why you shouldn't drive on winter tires in the summer months, . URL https://www.continental-tires.com/car/tire-knowledge/tire-change-fitting/changing-tires/winter-tires-in-summer. Accessed 2021-04-27.

[27] Raymond Brach and Matthew Brach. The tire-force ellipse (friction ellipse) and tire characteristics. *SAE Technical Paper 2011-01-0094*, 2011.

[28] VEHICO GmbH. ISO double lane change test, . URL https://www.vehico.com/index.php/en/applications/iso-lane-change-test. Accessed 2021-05-04.

[29] Chuang Su. *Integrated Experimental Methods and Machine Learning for Tire Wear Prediction*. PhD thesis, Virginia Polytechnic Institute and State University, 2019.